Neurochemical Research (2019) 44:1399–1409
https://doi.org/10.1007/s11064-018-02709-w

ORIGINAL PAPER

Segments in the Amyloid Core that Distinguish Hamster from Mouse Prion Fibrils

Howard C.-H. Shen[1,2] · Yung-Han Chen[1] · Yu-Sheng Lin[1,3] · Brett K.-Y. Chu[1,4] · Ching-Shin Liang[3] · Chien-Chih Yang[3] · Rita P.-Y. Chen[1,2]

Received: 27 July 2018 / Revised: 29 November 2018 / Accepted: 23 December 2018 / Published online: 2 January 2019

Abstract

Prion diseases are transmissible fatal neurodegenerative disorders affecting humans and other mammals. The disease transmission can occur between different species but is limited by the sequence homology between host and inoculum. The crucial molecular event in the progression of this disease is prion formation, starting from the conformational conversion of the normal, membrane-anchored prion protein (PrP^{C}) into the misfolded, β-sheet-rich and aggregation-prone isoform (PrP^{Sc}), which then self-associates into the infectious amyloid form called prion. Amyloid is the aggregate formed from one-dimensional protein association. As amyloid formation is a key hallmark in prion pathogenesis, studying which segments in prion protein are involved in the amyloid formation can provide molecular details in the cross-species transmission barrier of prion diseases. However, due to the difficulties of studying protein aggregates, very limited knowledge about prion structure or prion formation was disclosed by now. In this study, cross-seeding assay was used to identify the segments involved in the amyloid fibril formation of full-length hamster prion protein, SHaPrP(23–231). Our results showed that the residues in the segments 108–127, 172–194 (helix 2 in PrP^{C}) and 200–227 (helix 3 in PrP^{C}) are in the amyloid core of hamster prion fibrils. The segment 127–143, but not 107–126 (which corresponds to hamster sequence 108–127), was previously reported to be involved in the amyloid core of full-length mouse prion fibrils. Our results indicate that hamster prion protein and mouse prion protein use different segments to form the amyloid core in amyloidogenesis. The sequence-dependent core formation can be used to explain the seeding barrier between mouse and hamster.

Keywords Prion · Amyloid · Fibril · Hamster · Cross-β · Seeding

Introduction

Prion disease, also known as the transmissible spongiform encephalopathy (TSE), is a fatal neurodegenerative disease of sporadic, genetic, or infectious origin present in human and other mammalian species without any effective therapy available currently [1]. The infectious material of TSE is called prion, a special protease-resistant aggregation form produced from the misfolded prion protein PrP^{Sc}, which is converted from its normal cellular form PrP^{C} through an unclear mechanism. The discovery of prion challenges the central dogma of protein folding theory: one sequence→one structure. The structure of PrP^{C} contains three α-helices (144–153, 172–194 and 200–227) and two short antiparallel β-strands (129–131 and 161–164) in its C-terminal half, and its N-terminal half (sequence 23–120) does not contain any defined structure [2–4]. On the contrary, the exact structure of PrP^{Sc} is poorly understood. Owing to the

Special Issue: In Honor of Prof Anthony J Turner.

Electronic supplementary material The online version of this article (https://doi.org/10.1007/s11064-018-02709-w) contains supplementary material, which is available to authorized users.

✉ Rita P.-Y. Chen
pyc@gate.sinica.edu.tw

1 Institute of Biological Chemistry, Academia Sinica, No. 128, Sec. 2, Academia Rd, Nankang, Taipei 11529, Taiwan

2 Institute of Biochemical Sciences, National Taiwan University, Taipei 10617, Taiwan

3 Department of Biochemical Science and Technology, National Taiwan University, Taipei 10617, Taiwan

4 Department of Chemistry, National Taiwan University, Taipei 10617, Taiwan

aggregated nature of PrP^{Sc}, its structure has not been solved yet. We only know that prion has an amyloid fibril structure, in which the hydrogen bonds are formed between different molecules and align parallel to the direction of fibril propagation; therefore, the formed intermolecular β-sheets are called a cross-β structure. A decrease in α-helix content and an increase in β-sheet content were observed after the structural conversion based on the data from Fourier transform infrared spectroscopy [5] and circular dichroism spectroscopy [6]. Therefore, the $PrP^{C} \rightarrow PrP^{Sc}$ process is called an α-to-β or a coil-to-β structural conversion mechanism.

To gain insight into the structural conversion mechanism of prion formation, the potentially critical regions involved in the PrP^{Sc} formation have been studied for over two decades. The structure of amyloid fibrils, as insoluble aggregates, cannot be obtained using ordinary methods, such as X-ray crystallography and solution nuclear magnetic resonance spectroscopy. The structures of various fibrils formed by the recombinant prion protein of different lengths and species have been studied using a number of techniques, including hydrogen/deuterium exchange mass spectroscopy (HXMS) [7–11], hydrogen/deuterium exchange nuclear magnetic resonance spectroscopy [12], electron spin resonance (ESR) spectroscopy [13], solid state nuclear magnetic resonance spectroscopy (ssNMR) [14–20], cryo electron microscopy [21] and seeding assay [22, 23]. In studies on mouse, hamster and human recombinant full-length prion protein fibrils or the fibrils formed from their N-terminal truncated mutants, the region covering helix 2 and helix 3 was commonly reported as the loci where the α-to-β structural conversion takes place. Examples are sequences 182–212 [9] and 159–225 [8] by HXMS for mouse PrP(23–231); sequence 160–220 [13] by ESR and sequence 169–213 [7] by HXMS for human PrP(90–231); and sequence 163–223 [11] by HXMS for hamster PrP(90–231) and sequence 173–224 [17] by ssNMR for hamster PrP(23–231).

However, the finding of the truncated prion mutants at Y145 and Q160 in human prion disease reinforced the important role of the protein segment in front of three α-helices in the prion formation. A deletion PrP lacking residues 23–88 and 141–176, designated as PrP^{106}, was capable of forming infectious PrP^{Sc}-like molecules in transgenic mice [24], thus suggesting the importance of sequence 90–140. Shindoh et al. showed that the region 81–137 is critical for prion infectivity [25]. A peptide composed of hamster 109–141 or 119–136 could inhibit ^{35}S-labeled prion protein converted into PK-resistant aggregates in a cell-free conversion reaction [26, 27]. Overall, these above-mentioned studies proposed that the residues in the vicinity of PrP(108–144) could be involved in the intermolecular interactions between PrP-sen (protease-sensitive form of PrP) and PrP-res (protease-resistant form of PrP) that lead to fibrillation [28, 29]. This region has not been assigned as part of the amyloid core in full-length prion protein fibrils probably because the β-strand formed in this region is too short to exhibit significant protection in the hydrogen–deuterium exchange. Only in the fibrils formed from human Y145Stop and Q160Stop variants were the regions 112–115, 118–122 and 130–139 suggested to be the possible location of the β-strands in the cross-β structure of HuPrP (23–144) fibrils by ssNMR [14, 15]. The sequence 106–126 was found in the amyloid core of HuPrP(23–144) or HuPrP(23–159) fibrils by a seeding experiment [22].

In the current study, five peptides, namely, SHaPrP(108–144), SHaPrP(108–127), SHaPrP(128–144), SHaPrP(172–194) and SHaPrP(200–227), were synthesised by solid-phase peptide synthesis. The amyloidogenesis of the full-length recombinant SHaPrP protein and synthetic peptides was investigated in vitro by thioflavin T (ThT) assay. The cross-seeding capacity between the SHaPrP protein and peptides was used to identify the amyloid core region in the fibrils formed from the full-length hamster prion protein.

Materials and Methods

Peptide Synthesis

The prion peptides were synthesised by the Fmoc-polyamide method on a PS3 peptide synthesiser (Protein Technologies, Inc., Arizona, USA) [30]. Rink Amide AM resin was used as the solid support. Fmoc-amino-acid derivatives (0.6 mmole) purchased from Anaspec (California, USA) were coupled on the resin (0.1 mmole) using *O*-(1H-6-chlorobenzotriazole-1-yl)-1,1,3,3-tetramethyluronium (0.6 mmole) and 4.45% (v/v) *N*-methyl morpholine in dimethylformamide (DMF). The Fmoc cleavage step was performed using 20% (v/v) piperidine in DMF. N-terminal acetylation was performed using four equivalents of acetic anhydride instead of an amino acid derivative in the final synthetic step. Side-chain deprotection and peptide cleavage from the resin were performed by stirring the resin in a mixture of trifluoroacetic acid/water/ethanedithiol/triisopropylsilane (94/2.5/2.5/1, v/v) at room temperature for 2 h. After the cleavage reaction was completed, the resin was removed by passing the reaction mixture through a G2 glass funnel. The peptides in the filtrate were precipitated by adding three volumes of ice-cold methyl t-butyl ether (MTBE). The precipitate was collected by centrifugation at 3000 g for 20 min at 4 °C, washed twice with ice-cold MTBE and dried under vacuum. The crude peptides were purified by reverse-phase high-performance liquid chromatography (RP-HPLC) using a C18 column (4.6 mm × 250 mm, Shiseido, Japan) and identified by matrix-assisted laser desorption ionization time-of-flight (MALDI-TOF) mass spectroscopy (micro MX™, Waters,

USA). The eluted peptide solution was collected, lyophilised and stored in a − 30 °C freezer. These synthesised peptides have acetylation at the N-terminus and amidation at the C-terminus to mimic their status in protein without electrostatic interaction at the two ends.

Expression and Purification of Full-Length SHaPrP(23–231)

To express SHaPrP(23–231) in *Escherichia coli*, the plasmid pET28a-SHaPrP(23–231)-containing hamster gene with codon optimisation by OptimiumGene™ Codon Optimisation Analysis was synthesised by GenScript (New Jersy, USA). The translated protein had 210 residues, corresponding to the hamster prion protein sequence 23–231 plus an extra Gly at its N-terminus with a molecular mass of 23,028 Da. The Met residue coded by the initiation codon was cleaved by methionine aminopeptidase in *E. coli* [31, 32]. The plasmid was transformed into *E. coli* BL21 Star (DE3) (Invitrogen, California, USA). Compared with that of the plasmid inserted with the original hamster *PRNP* gene, the yield of the protein obtained from this codon-optimised plasmid was at least six-folds higher.

To express SHaPrP(23–231), an overnight culture was used to inoculate fresh Luria–Bertani medium containing kanamycin (40 µg/mL), and the cells were grown at 37 °C with vigorous shaking (250 rpm) until $O.D._{600}$ reached 0.6. Protein expression was induced by adding isopropyl β-D-1-thiogalactopyranoside to a final concentration of 1 mM, and the culture was grown for an additional 6 h. Then, the cells were harvested by centrifugation at 6000 g at 4 °C for 15 min. The cell pellet was resuspended in the cell lysis buffer (50 mM Tris, 100 mM NaCl and pH 8.0 at about 9 mL/g cell), and cell lysis was conducted by incubating with 0.1 × CelLyticB, 0.15 mg/mL lysozyme, 25 µg/mL DNaseI, 7 mM $MgCl_2$ and 1 mM phenylmethylsulfonyl fluoride (PMSF) for 30 min at room temperature with stirring.

The protein purification protocol was modified from our previous report [33]. In brief, inclusion bodies were collected from the cell lysate by centrifugation at 20,000 g for 30 min at 4 °C and resuspended in the IMAC buffer A (8 M urea, 100 mM Na_2HPO_4, 10 mM Tris-HCl, 10 mM GSH and pH 8.0) with rotation at 40 rpm for 2 h at room temperature. The supernatant containing the solubilised proteins was collected by centrifugation at 30,000 g for 25 min at 4 °C, filtered through a 0.45 µM Millipore syringe filter and loaded onto the prepacked nickel-chelating Fast Flow Sepharose column (GE Healthcare, Illinois, USA). After washing with 5 column volumes of the IMAC buffer A, the target protein was eluted with buffer B (8 M urea, 100 mM Na_2HPO_4, 10 mM Tris-HCl, 10 mM glutathione and pH 4.5). Desalting was performed using a HiPrep 26/10 column prepacked with Sephadex G-25 Superfine gel (GE Healthcare, USA) on the ÄKTAprime plus FPLC system (GE Healthcare, Illinois, USA) with a desalting buffer (6 M urea, 0.1 M Tris-HCl and pH 7.5). Disulphide bond formation was conducted by adding 5 mM ethylenediaminetetraacetic acid and 0.2 mM glutathione disulphide to the eluted protein fraction and incubating the solution for 18 h at 4 °C. The oxidised protein was purified by RP-HPLC on a C5 column (Discovery BIO Wide Pore C5, 10 µm, 25 cm × 10.0 mm, Supelco, USA). Protein identification was examined by electrospray ionisation time-of-flight (ESI-TOF) mass spectrometry. The eluted protein was lyophilised and stored at − 30 °C.

ThT Binding Assay of Amyloidogenesis

Amyloid fibril formation, including the spontaneous and seeded amyloidogenesis of PrP protein and peptides, was monitored using the ThT binding assay. The fibril solution was mixed with the same volume of 200 µM ThT in 140 mM KCl and 100 mM sodium phosphate buffer (pH 8.5) for 1 min at room temperature. Fluorescence spectra from 450 nm to 600 nm were measured in a 3 mm path–length rectangular cuvette on a FP-750 fluorescence spectrometer (JASCO, Japan) with excitation at 442 nm. For the protein fibrils, the excitation wavelength was changed to 420 nm to avoid the interference of light scattering. The excitation and emission slits were set to 5 nm and 10 nm, respectively.

Transmission Electron Microscopy (TEM)

The amyloid fibril solution was loaded on carbon-coated 300-mesh copper grids, incubated for 3 min and then stained with freshly filtered 2% uranyl acetate for 15 s. After the grid was dried, the samples were viewed on the FEI Tecnai G2 TF20 Super TWIN electron microscope (Thermo Fisher Scientific, Oregon, USA).

Spontaneous Amyloid Fibril Formation of Hamster Prion Protein and Peptides

SHaPrP(23–231) was dissolved in 6 M GdnHCl as a 150 µM stock solution. To form amyloid fibrils, SHaPrP(23–231) stock was mixed with the buffer to make a final protein concentration of 25 µM in 1 × phosphate-buffered saline (PBS), 1M GdnHCl and 3M urea (pH 7.4). The final volume of the solution is 1 mL. The solution was incubated at 37 °C with vigorous shaking (250 rpm).

SHaPrP(108–144), SHaPrP(108–127), SHaPrP(128–144) and SHaPrP(172–194) were dissolved in deionised water as stock solutions. SHaPrP(200–227) formed fibrils too fast, and thus the stock solution was made in 60% acetonitrile solution. Peptide stocks were diluted with an equal volume of 2 × peptide amyloidogenesis buffer (20 mM phosphate

buffer, 792 mM NaCl and 0.02% NaN_3; pH 7.5), and the solutions were incubated at 37 °C without shaking [19].

The lag time of amyloidogenesis was obtained by fitting the kinetic data using the following equation: F = A + B/(1 + e^(k*($t_{1/2}$ − t))), where A is the signal during the lag phase, B is the signal difference between the lag phase and the post-transition plateau, t is the time, $t_{1/2}$ is the time required for the half-completion of the fibrillation process and k is the rate constant of fibril growth (h^{-1}). Lag time is equal to $t_{1/2} - 2/k$.

Seed Preparation and Seeding Assay

The amyloid fibril solutions generated from the SHaPrP peptides or full-length protein were spun down by centrifugation at 19,000 g for 30 min at room temperature. The amount of peptides or protein remaining in the solution was measured by RP-HPLC. The amount of peptides or protein in fibrils was calculated by deducting the remaining monomer amount in the solution from the original concentration. The precipitated fibrils were re-suspended in deionised water. To acquire a nearly homogeneous seed, the fibril solution was fragmented with 20 (for peptide fibrils) or 60 cycles (for protein fibrils) of intermittent pulses (five pulses of 0.6 s each with a 5 s interval between each cycle) by an ultrasonic processor (UP200H, Hielscher Ultrasonic GmbH, Teltow, Germany) equipped with a 1 mm microtip immersed in the sample. The power was set to 20%. For the seeding reaction, different amounts of seed were added to the monomer solution to make the final volume as 1 mL. The process of amyloidogenesis was monitored at different incubation times by the ThT binding assay.

To prepare a proteinase K (PK)-digested seed, the SHaPrP(23–231) fibrils were spun down at 19,000 g for 30 min, re-suspended in deionised water and reacted with PK (molar ratio of enzyme to substrate was 1–50) at 37 °C for 1 h with 250 rpm of shaking. To terminate the reaction, PMSF was added to the final PMSF concentration of 5 mM, and the solution was heated at 70 °C for 15 min. The PK-digested fibrils were spun down, re-suspended in deionised water and then used for preparing the seed as described above.

Results

Spontaneous Amyloid Fibril Formation of the Hamster Full-Length Recombinant Prion Protein and Prion Peptides

The sequences of the SHaPrP peptides used in this study are shown in Fig. 1. The kinetics of amyloidogenesis of the hamster prion protein SHaPrP(23–231) and five peptides, namely, SHaPrP(108–144), SHaPrP(108–127), SHaPrP(128–144), SHaPrP(172–194) and SHaPrP(200–227), was monitored by the enhanced fluorescence emission of ThT upon binding to the hydrophobic cavities in the amyloid fibrils [34–36]. The full-length prion protein gradually formed amyloid fibrils in a partial denaturing condition. Its fluorescence emission spectra at different incubation times are shown in Fig. 2a, and the kinetic curves of the amyloidogenesis of three independent samples are illustrated in Fig. 2b. SHaPrP(23–231) in PBS (pH 7.4), 1 M GdnHCl and 3 M urea had a lag time of about 60 h, and fibril propagation reached equilibrium after 120 h (Fig. 2b). Conversely, prion peptides could transform into fibrils without the help of any denaturant (Fig. 3). All five prion peptides could form amyloid fibrils in the same buffer (10 mM phosphate buffer, 396 mM NaCl and 0.01% NaN_3) [19]. SHaPrP(108–127), which has a special palindromic sequence AGAAAAGA, had the lowest amyloidogenic property compared with the other prion peptides, and a much higher peptide concentration (800 μM) was required for the fibril formation of SHaPrP(108–127) (green curve in Fig. 3a). Conversely, SHaPrP(172–194) and SHaPrP(200–227), the segments corresponding to the helix 2 and helix 3 of PrP^C, respectively, were prone to amyloid formation. The nucleation of these two peptides was so fast, and we could hardly find the nucleation phase in their kinetic curves even when the peptide concentration was reduced (Fig. 3b, c). Specifically, SHaPrP(200–227) is the most amyloidogenic peptide. Its stock solution had to be prepared in

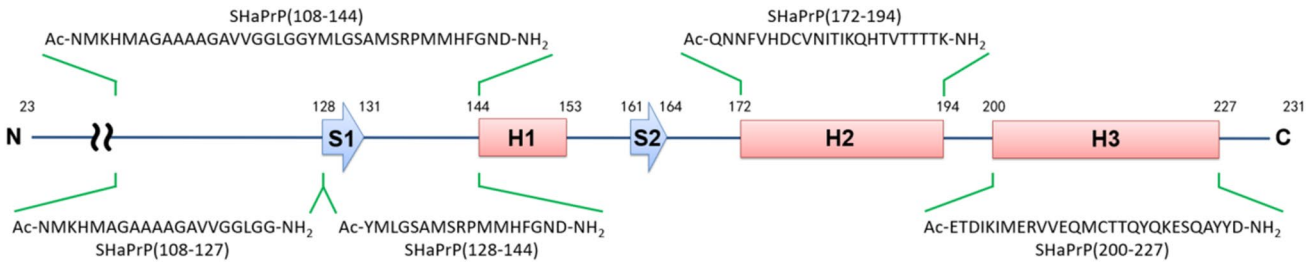

Fig. 1 Sequence and location of the five prion peptides used in this study. The three α-helices are marked as H1, H2 and H3 in red boxes. The two β-strands are marked as S1 and S2 in blue arrows. (Color figure online)

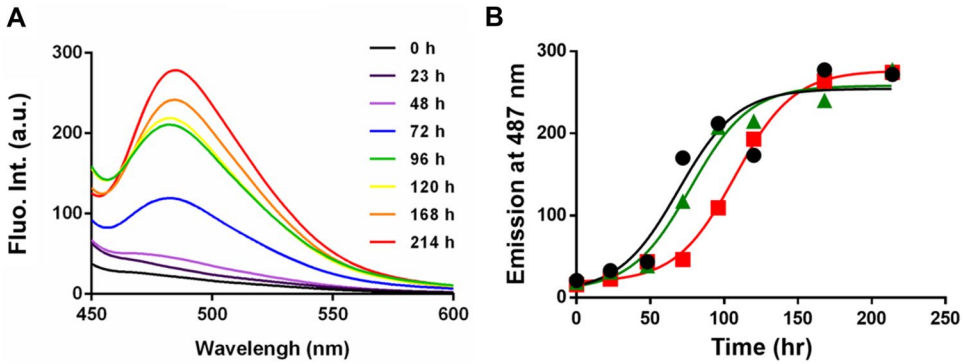

Fig. 2 Spontaneous amyloidogenesis of the recombinant hamster prion protein SHaPrP(23–231). SHaPrP(23–231) (22 μM) in 1 × PBS, 1M GdnHCl and 3M urea (pH 7.4) was incubated at 37 °C with vigorous shaking. **a** Fluorescence spectra recorded at different incubation times. **b** Kinetic curves from three independent samples. (Color figure online)

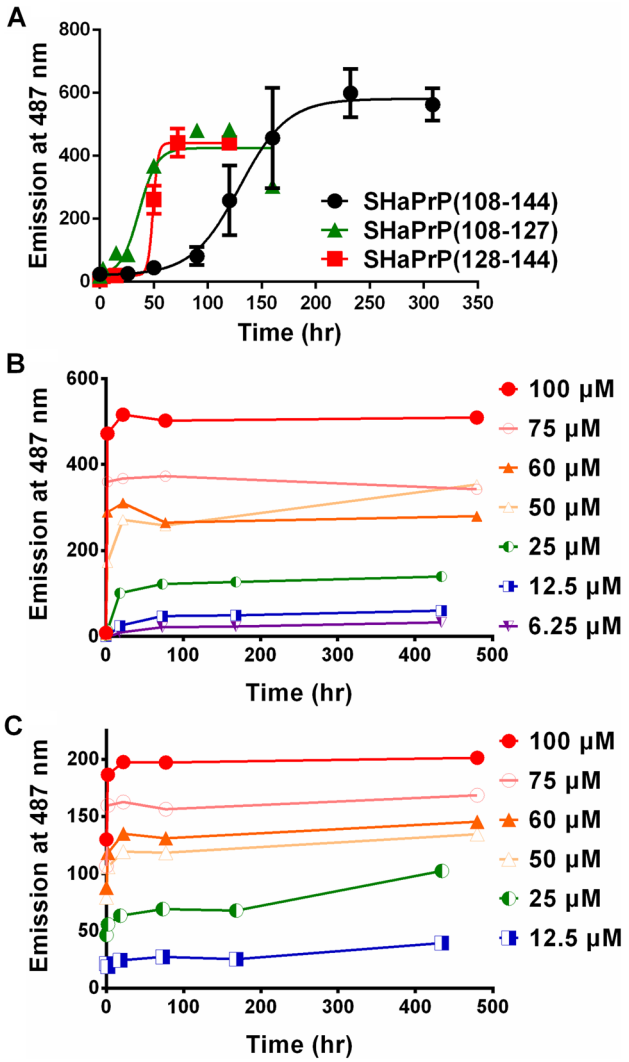

Fig. 3 Spontaneous amyloidogenesis of synthetic hamster prion peptides. The peptides were incubated in 10 mM phosphate buffer, 396 mM NaCl and 0.01% NaN_3 (pH 7.5) at 37 °C. **a** Averaged kinetics curves of 150 μM SHaPrP(108–144), 800 μM SHaPrP(108–127) and 150 μM SHaPrP(128–144) from three independent samples. **b** Kinetic curves of the different concentrations of SHaPrP(172–194). **c** Kinetic curves of the different concentrations of SHaPrP(200–227). (Color figure online)

60% acetonitrile to avoid aggregation before incubation began. The fibril morphology of the hamster protein and peptide fibrils was revealed by TEM (Fig. 4).

Seeding Capacity of Amyloidogenesis: Using SHaPrP Peptide Fibrils as a Seed and SHaPrP(23–231) as a Substrate

If the SHaPrP peptides and full-length SHaPrP(23–231) use the same segment to form the cross-β structure in amyloidogenesis, the fibrils generated from peptides will be able to serve as a template (seed) to induce monomeric SHaPrP(23–231) to polymerise and form amyloid fibrils. The amyloid fibrils of the SHaPrP protein and peptides, generated from spontaneous amyloidogenesis, were collected through centrifugation, and the amount of the molecules in fibrils was quantified by deducting the remaining monomer concentration from the original concentration. To avoid the presence of large fibril tangles in a seed, the collected fibrils were fragmented (seed length was 50–200 nm) by sonication (Fig. S1). As shown in Fig. 5a, the SHaPrP(23–231) seed can efficiently initiate the fibrillation of the SHaPrP(23–231) monomer. In the same condition, SHaPrP(23–231) can be seeded by the SHaPrP(108–144) seed, the SHaPrP(108–127) seed, the SHaPrP(172–194) seed and the SHaPrP(200–227) seed as well (Fig. 5b, c, e and f). Among them, the SHaPrP(172–194) seed is the most efficient seed because lag time can hardly be detected. This finding indicates that the segments of SHaPrP(108–144), SHaPrP(108–127), SHaPrP(172–194) and SHaPrP(200–227) could be involved in the amyloid core of the full-length SHaPrP(23–231) amyloidogenesis.

The only exception is SHaPrP(128–144). The SHaPrP(128–144) seed cannot seed the fibrillation of the SHaPrP(23–231) monomer (Fig. 5d). This finding is not consistent with that of a previous study on the amyloidogenesis of mouse prion protein, in which the full-length mouse prion protein was seeded by the peptides mPrP(107–143) and mPrP(127–143) but not by mPrP(107–126) (mouse and hamster sequence numbers have one residue difference) [23].

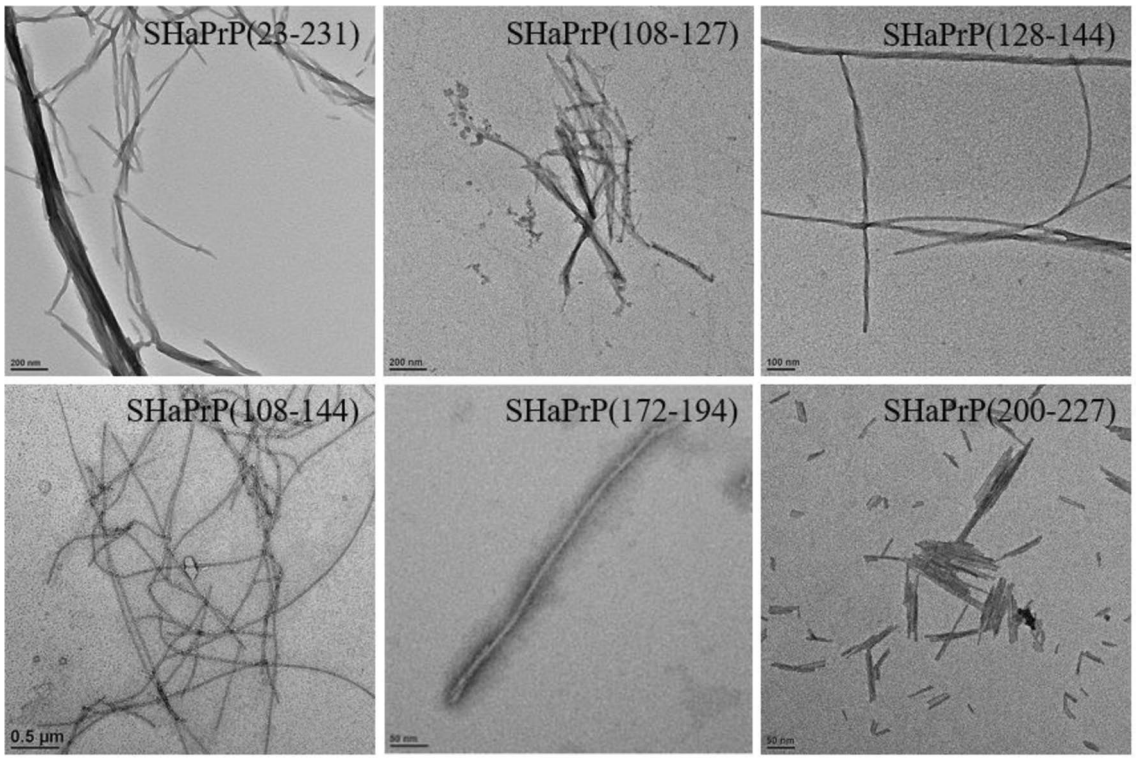

Fig. 4 TEM images of the fibrils formed of the hamster prion protein SHaPrP(23–231) and peptides SHaPrP(108–144), SHaPrP(108–127), SHaPrP(128–144), SHaPrP(172–194) and SHaPrP(200–227)

Seeding Capacity of Amyloidogenesis: Using SHaPrP(23–231) Fibrils as a Seed and SHaPrP Peptides as a Substrate

The finding that the SHaPrP(108–144), SHaPrP(108–127), SHaPrP(172–194) and SHaPrP(200–227) fibrils can induce the fibrillation of SHaPrP(23–231) suggests SHaPrP(23–231) can use these segments as a template to form the cross-β structure in the seeding experiment. If the spontaneously converted SHaPrP(23–231) fibrils do use these segments to form the cross-β structure in its amyloid core, the SHaPrP(23–231) fibrils will be able to induce the fibrillation of these four peptides as well. Thus, we examined the amyloidogenesis of the SHaPrP peptides seeded by their own fibrils or the SHaPrP(23–231) fibrils. SHaPrP(108–144), SHaPrP(108–127) and SHaPrP(128–144) could be efficiently seeded by its own fibrils (Fig. 6a–c). Interestingly, the addition of the SHaPrP(23–231) seed did not shorten the lag time for the fibrillation of SHaPrP(108–144) and SHaPrP(108–127) (blue and yellow curves in Fig. 6d, e, respectively). On the contrary, the seed inhibited the nucleation of SHaPrP(108–127) and extended the lag time. As the amyloid core region in the SHaPrP(23–231) seed could be buried and shielded by the unstructured part of the protein, we used PK to remove the protease-sensitive region of the SHaPrP(23–231) fibrils. The SHaPrP(23–231) PK-digested seed was prepared by treating the seed with PK for 1 h at 37 °C. After the treatment, the SHaPrP(23–231) PK-digested seed could efficiently induce the fibrillation of SHaPrP(108–144) (green and red curves in Fig. 6d). Using the seed titration method, Lee and Chen previously proposed that the amyloid propagation surface of the mouse and hamster prion peptides with the sequence 108–144 was determined depending on the residue at position 139 [37]. When residue-139 is Ile (the mouse sequence), the sequence homology at the C-terminal half of the peptide becomes important for efficient seeding. When residue-139 is Met (the hamster sequence), the sequence homology at its N-terminal half of the peptide determines its seeding efficiency. Thus, we used the same PK-digested seed to induce the amyloidogenesis of the SHaPrP(108–127) and SHaPrP(128–144) monomers. The results for SHaPrP(108–127) were similar to those for SHaPrP(108–144) (Fig. 6e). The SHaPrP(23–231) PK-digested seed could efficiently induce the amyloid formation of the SHaPrP(108–127) monomer, and the lag time was too short to be detected. In the seeding assay using SHaPrP(128–144) as a monomer, neither the SHaPrP(23–231) seed nor the SHaPrP(23–231) PK-digested seed had the seeding ability (Fig. 6f). The results are consistent with our assumption and suggest that the segment 108–127 is in the amyloid core of the SHaPrP(23–231) fibrils but the segment 128–144 is not.

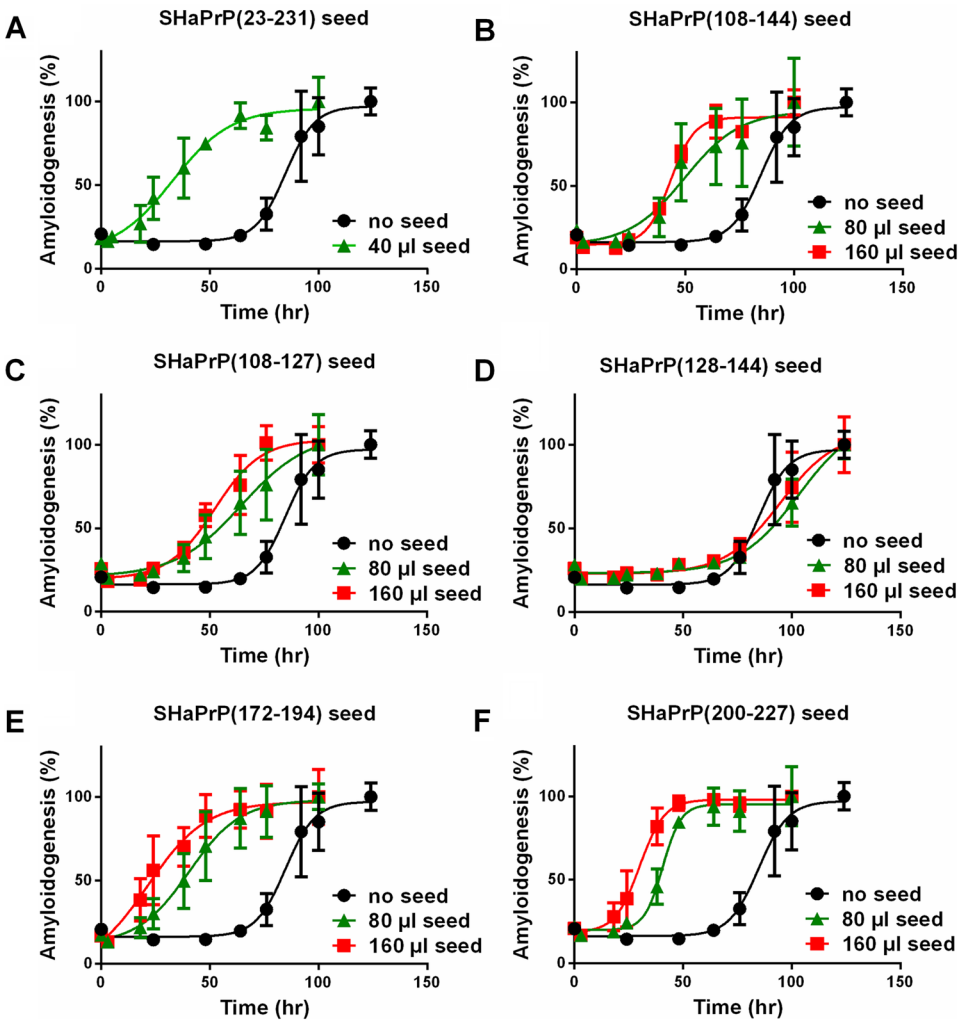

Fig. 5 Seeding efficacies of the SHaPrP peptide seed in the amyloidogenesis of SHaPrP(23–231). SHaPrP(23–231) (25 µM) incubation in 1 × PBS, 1M GdnHCl, 3M urea and pH 7.4 at 37 °C with shaking by adding a buffer or sonicated **a** SHaPrP(23–231) seed, **b** SHaPrP(108–144) seed, **c** SHaPrP(108–127) seed, **d** SHaPrP(128–144) seed, **e** SHaPrP(172–194) seed and **f** SHaPrP(200–227) seed. The kinetic curves are the averaged results from three independent samples, and the error bars are shown. The amount of molecule in the fibril form of the seed is 67 pmole per µL for the SHaPrP(23–231) seed, 15.25 pmole per µL for the SHaPrP(108–144) seed, 14.07 pmole per µL for the SHaPrP(108–127) seed, 25.0 pmole per µL for the SHaPrP(128–144) seed, 1.75 pmole per µL for the SHaPrP(172–194) seed and 1.87 pmole per µL for the SHaPrP(200–227) seed. The kinetic curves of the fibril formation were monitored by the ThT binding assay and normalized according to the fluorescence emission at the final incubation time. (Color figure online)

For SHaPrP(172–194) and SHaPrP(200–227), we could not conduct a seeding experiment because no lag time could be detected in the amyloidogenesis kinetics of these two peptides. We attempted to change the buffer conditions, but nucleation remained too fast (Figs. S2 and S3).

Discussion

In prion research, a key molecular event is the conformational change from the cellular prion protein PrP^{C} into the misfolded and pathogenic isoform, PrP^{Sc}. Many research groups have attempted different methods to solve the conversion mechanism. However, in the structural studies of full-length prion protein fibrils, the role of the 108–144 region in the structural conversion was hardly defined.

In this study, we used the same buffer and incubation conditions to compare the amyloidogenic property of the five prion peptides. All these five peptides can form amyloid fibrils in the same condition. The nucleation of SHaPrP(172–194) and SHaPrP(200–227) was too fast to show the lag phase in their fibrillation kinetics. Their strong amyloidogenic propensity echoed the finding that helix 2 and helix 3 were likely involved in the structural conversion of prion fibril formation in vivo and in vitro [8, 17, 21, 38]. SHaPrP(108–127) needed a much higher monomer concentration (800 µM) to initiate fibrillation. This result is similar to that of mouse prion peptides [23], as it suggests that the segment 108–127 has a higher energy barrier for nucleation. This segment contains the palindromic sequence AGAAAA GA, which can form the cross-β structure in peptide 109–122 [20]. Compared with the other peptides, SHaPrP(108–127) has fewer hydrophobic residues, thus increasing its thermodynamic solubility.

The seeding effect is an important feature for the nucleation-dependent polymerization of amyloid formation and is the reason why a protein can be infectious. Yamaguchi et al. reported that the amyloid formation of the full-length mouse prion protein could be seeded by the mouse H2 peptide (sequence 171–193) and the H3 peptide (sequence

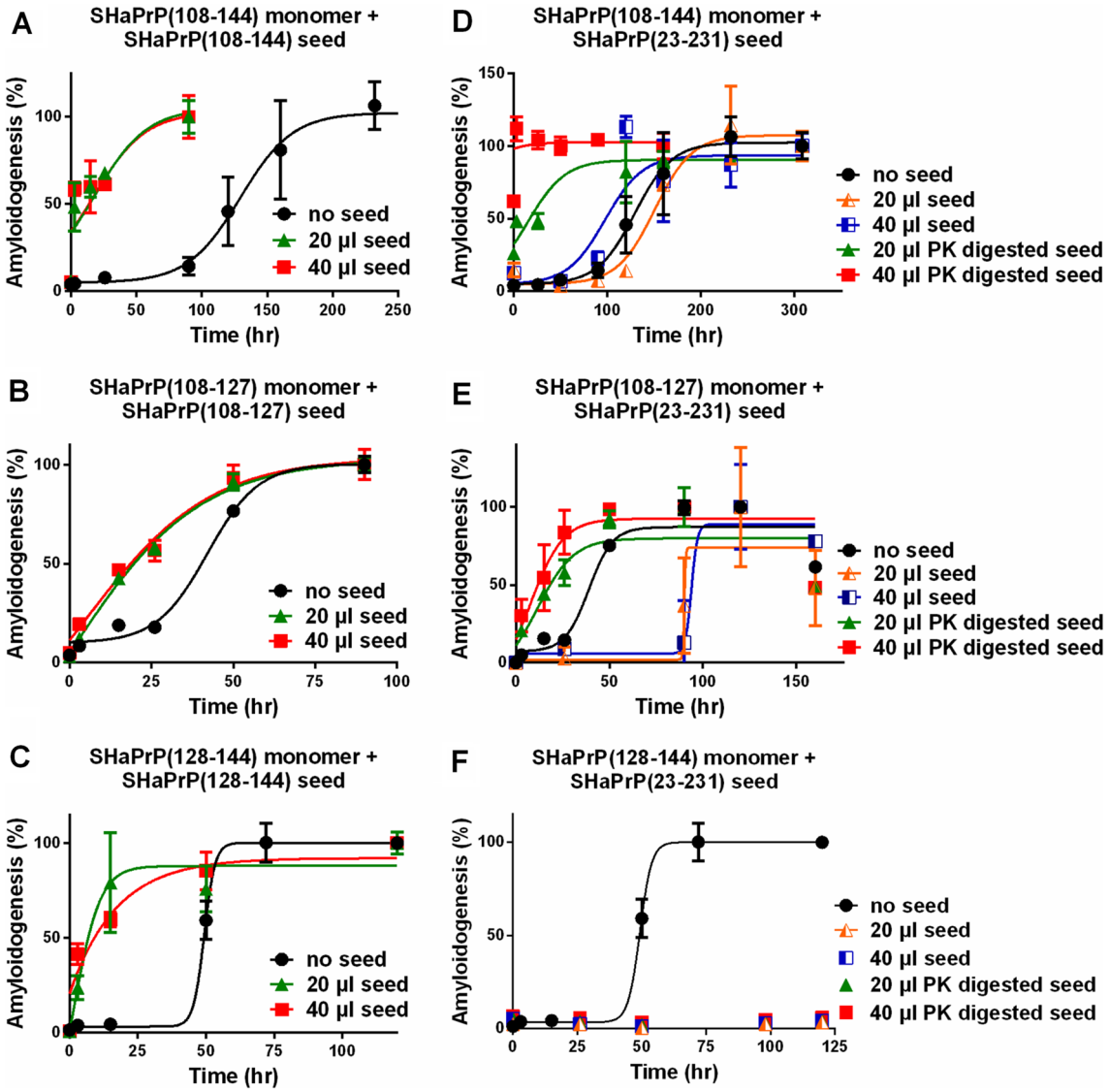

Fig. 6 Seeding efficacies of various SHaPrP peptide seeds in the amyloidogenesis of SHaPrP(23–231). SHaPrP(108–144) (150 µM), SHaPrP(108–127) (800 µM) and SHaPrP(128–144) (150 µM) were incubated in 10 mM phosphate buffer, 396 mM NaCl and 0.01% NaN_3 (pH 7.5) at 37 °C with or without their own fibril seed (**a–c**) or seeded by the SHaPrP(23–231) seed and SHaPrP(23–231) PK-digested seed (**d–f**). The amount of molecules in the fibril form of the seed is 9.88 pmole per µL for the SHaPrP(108–144) seed, 63.31 pmole per µL for the SHaPrP(108–127) seed, 10.07 pmole per µL for the SHaPrP(128–144) seed and 10.82 pmole per µL for the SHaPrP(23–231) seed. (Color figure online)

199–226) [39]. In our seeding study, SHaPrP(172–194) and SHaPrP(200–227) can also induce the amyloidogenesis of the full-length hamster prion protein, supporting the important role of these two segments in the α-to-β conversion process either in mouse or hamster. However, contrasting results were found for hamster and mouse in the region of 108–144. Chatterjee et al. reported that the mPrP(107–143) and mPrP(127–143) seeds could induce the fibril formation of the full-length mouse prion protein, but the fibrils formed by mPrP(107–126) could not [23]. In our seeding assay, the SHaPrP(23–231) monomer could be seeded by the SHaPrP(108–144) seed and the SHaPrP(108–127) seed but not by the SHaPrP(128–144) seed (Fig. 5). The SHaPrP(128–144) seed did not work in the seeding assay is not due to the stability of the SHaPrP(128–144) fibrils in the partially denaturing condition since the β-structure signal of the SHaPrP(128–144) fibrils can still be observed in the amyloidogenesis buffer after long term incubation (Fig. S4). Moreover, only the SHaPrP(108–144) and SHaPrP(108–127) monomers could be seeded by the PK-digested SHaPrP(23–231) seed and the SHaPrP(128–144) monomer could not (Fig. 6). These findings suggest at least

four segments (108–127, 128–144, 172–194 and 200–227) in the prion protein have their own amyloidogenic propensity, but not all of them can be found in the amyloid core of the prion protein fibrils. The sequence homology at position-139 between inoculum and host strongly affected the interspecies transmissibility between hamster and mouse PrP [37, 40, 41], and the sequence difference led to different fibril structures [42, 43]. To date, no structural data have been provided to prove whether the full-length mouse and hamster prion proteins use different segments to form their amyloid cores or not. In this study, we provide the evidence to demonstrate the different roles of the segments 108–127 and 128–144 in the amyloidogenesis of the hamster and mouse prion protein in the in vitro fibril formation system.

In addition, one interesting phenomenon we observed is the extension of the lag time in the amyloidogenesis kinetic of SHaPrP(108–127) when the SHaPrP(23–231) fibrils were added as a seed (Fig. 6e). Because the PK-treated SHaPrP(23–231) seed was prepared from the SHaPrP(23–231) seed, the seed amount was no more than the amount of the SHaPrP(23–231) seed. Compared with the strong seeding effect of the PK-treated SHaPrP(23–231) seed, this result suggested that the PK-sensitive part in the SHaPrP(23–231) seed had the interference effect in the nucleation step of SHaPrP(108–127). The interference effect is more prominent in seeding SHaPrP(128–144) monomer (Fig. 6f) since no ThT fluorescence increase can be detected (Fig. S5A). Using circular dichroism (CD) spectroscopy we found that the CD spectrum of the solution containing SHaPrP(128–144) monomer plus PK-treated SHaPrP(23–231) seed had less negative ellipticity after incubation, indicating the peptide might aggregate (Fig. S5B). Indeed, amorphous aggregates could be found under TEM (Fig. S5C). We surmise that the segment 128–144 might be flexible in the protein seed. Therefore, instead of serving as a template for fibril extension, the protein seed interacted with SHaPrP(128–144) and promote another aggregation pathway. When the PK-digested SHaPrP(23–231) seed was further treated with trypsin, a peptide fragment corresponding to the residues 117–136, can be identified by the MS/MS study (Fig. S6). The data suggested that proteinase K might cut between residues 116 and 117. The template that assisted SHaPrP(108–127) fibrillation might reside in the segment 117–127 (sequence AAGAVVGGLGG).

Up to now, four structural models have been proposed: (1) the parallel in-register intermolecular β-sheet (PIRIBS) model [13, 44]; (2) the four-rung β-solenoid model [21, 45–47]; (3) the β-spiral model [28]; and (4) the left-handed β-helix model [48]. Since no α-helical structure can be detected on brain-derived prion or recombinant PrP amyloid, the possibilities of the latter two models have been ruled out [10]. Wille et al. have reported that the brain-derived prion and recombinant PrP amyloid fibrils have distinct fibre diffraction patterns [45]. The four-rung β-solenoid model was proposed based on the studies on the brain-derived prion by X-ray fiber diffraction [45] and cryo EM [21]. In this model, only the β-strand on the upper or lowermost rungs can serve as a template in the seeding studies. On the contrary, the PIRIBS model was proposed based on the studies on the recombinant PrP amyloid fibrils by ESR spectroscopy [13] and ssNMR [44]. In this model, all the β-strands stacks on top of the preceding molecule and can template either an incoming protein monomer or the corresponding peptide segments. The strong spin exchange effect for the fibrils with a spin labled in the region of 160–220 suggested that the in-vitro prepared PrP fibrils can not be the four-rung β-solenoid structure [13]. Our seeding results did not fit with the four-rung β-solenoid model but matched well with the PIRIBS model. All the data suggested the structural difference between the naturally formed prion fibrils and the PrP amyloid fibrils formed in a partially denaturing condition. Most importantly, the current data imply that the same protein can aggregate into different misfolded structure depending on the environment.

In conclusion, a seeding experiment was used to probe the cross-β structure of in vitro prepared hamster prion protein fibrils. Our findings indicate that the prion protein sequence can affect the structural conversion mechanism that is promoted under a partial denaturing condition.

Acknowledgements The TEM images were obtained with the assistance of Mr. Tai-Lang Lin from the core facility of the Institute of Cellular and Organismic Biology, Academia Sinica. Mass spectra were acquired from three mass spectrometry facilities in Academia Sinica. Protein identification by ESI-TOF was conducted in the mass spectrometry facility of the Institute of Chemistry. Peptide identification by MALDI-TOF was conducted in the mass spectrometry facility of the Institute of Molecular Biology. The MS/MS study by LTQ Orbitrap was performed in the Academia Sinica Common Mass Spectrometry Facility for proteomics and protein modification analysis located at the Institute of Biological Chemistry, supported by Academia Sinica Core Facility and Innovative Instrument Project (AS-CFII-108-107). This work was funded by the Ministry of Science and Technology (MOST) of Taiwan (MOST 105-2119-M-001-028).

Compliance with Ethical Standards

Conflict of interest The authors declare no conflict of interest.

References

1. Prusiner SB (1998) Prions. Proc Natl Acad Sci USA 95:13363–13383
2. Donne DG, Viles JH, Groth D, Mehlhorn I, James TL, Cohen FE, Prusiner SB, Wright PE, Dyson HJ (1997) Structure of the recombinant full-length hamster prion protein PrP(29–231): the N terminus is highly flexible. Proc Natl Acad Sci USA 94:13452–13457

3. Riek R, Hornemann S, Wider G, Glockshuber R, Wuthrich K (1997) NMR characterization of the full-length recombinant murine prion protein, mPrP(23–231). FEBS Lett 413:282–288
4. Riek R, Hornemann S, Wider G, Billeter M, Glockshuber R, Wuthrich K (1996) NMR structure of the mouse prion protein domain PrP(121–231). Nature 382:180–182
5. Pan K, Baldwin M, Nguyen J, Gasset M, Serban A, Groth D, Mehlhorn I, Huang Z, Fletterick R, Cohen F, Prusiner S (1993) Conversion of a-helices b-sheets features in the formation of the scrapie prion proteins. Proc Natl Acad Sci USA 90:10962–10966
6. Safar J, Roller P, Gajdusek D, Gibbs C Jr (1993) Conformational transitions, dissociation, and unfolding of scrapie amyloid (prion) protein. J Biol Chem 268:20276–20284
7. Lu X, Wintrode PL, Surewicz WK (2007) b-Sheet core of human prion protein amyloid fibrils as determined by hydrogen/deuterium exchange. Proc Natl Acad Sci USA 104:1510–1515
8. Singh J, Udgaonkar JB (2013) Dissection of conformational conversion events during prion amyloid fibril formation using hydrogen exchange and mass spectrometry. J Mol Biol 425:3510–3521
9. Nazabal A, Hornemann S, Aguzzi A, Zenobi R (2009) Hydrogen/deuterium exchange mass spectrometry identifies two highly protected regions in recombinant full-length prion protein amyloid fibrils. J Mass Spectrom 44:965–977
10. Smirnovas V, Baron GS, Offerdahl DK, Raymond GJ, Caughey B, Surewicz WK (2011) Structural organization of brain-derived mammalian prions examined by hydrogen-deuterium exchange. Nat Struct Mol Biol 18:504–506
11. Smirnovas V, Kim JI, Lu X, Atarashi R, Caughey B, Surewicz WK (2009) Distinct structures of scrapie prion protein (PrPSc)-seeded versus spontaneous recombinant prion protein fibrils revealed by hydrogen/deuterium exchange. J Biol Chem 284:24233–24241
12. Kuwata K, Matumoto T, Cheng H, Nagayama K, James TL, Roder H (2003) NMR-detected hydrogen exchange and molecular dynamics simulations provide structural insight into fibril formation of prion protein fragment 106–126. Proc Natl Acad Sci USA 100:14790–14795
13. Cobb NJ, Sonnichsen FD, McHaourab H, Surewicz WK (2007) Molecular architecture of human prion protein amyloid: a parallel, in-register b-structure. Proc Natl Acad Sci USA 104:18946–18951
14. Helmus JJ, Surewicz K, Apostol MI, Surewicz WK, Jaroniec CP (2011) Intermolecular alignment in Y145Stop human prion protein amyloid fibrils probed by solid-state NMR spectroscopy. J Am Chem Soc 133:13934–13937
15. Helmus JJ, Surewicz K, Nadaud PS, Surewicz WK, Jaroniec CP (2008) Molecular conformation and dynamics of the Y145Stop variant of human prion protein in amyloid fibrils. Proc Natl Acad Sci USA 105:6284–6289
16. Helmus JJ, Surewicz K, Surewicz WK, Jaroniec CP (2010) Conformational flexibility of Y145Stop human prion protein amyloid fibrils probed by solid-state nuclear magnetic resonance spectroscopy. J Am Chem Soc 132:2393–2403
17. Tycko R, Savtchenko R, Ostapchenko VG, Makarava N, Baskakov IV (2010) The alpha-helical C-terminal domain of full-length recombinant PrP converts to an in-register parallel beta-sheet structure in PrP fibrils: evidence from solid state nuclear magnetic resonance. Biochemistry 49:9488–9497
18. Cheng HM, Tsai TW, Huang WY, Lee HK, Lian HY, Chou FC, Mou Y, Chan JC (2011) Steric zipper formed by hydrophobic peptide fragment of Syrian hamster prion protein. Biochemistry 50:6815–6823
19. Lin NS, Chao JC, Cheng HM, Chou FC, Chang CF, Chen YR, Chang YJ, Huang SJ, Chan JC (2010) Molecular structure of amyloid fibrils formed by residues 127 to 147 of the human prion protein. Chemistry 16:5492–5499
20. Lee SW, Mou Y, Lin SY, Chou FC, Tseng WH, Chen CH, Lu CY, Yu SS, Chan JC (2008) Steric zipper of the amyloid fibrils formed by residues 109–122 of the Syrian hamster prion protein. J Mol Biol 378:1142–1154
21. Vazquez-Fernandez E, Vos MR, Afanasyev P, Cebey L, Sevillano AM, Vidal E, Rosa I, Renault L, Ramos A, Peters PJ, Fernandez JJ, van Heel M, Young HS, Requena JR, Wille H (2016) The structural architecture of an infectious mammalian prion using electron cryomicroscopy. PLoS Pathog 12:e1005835
22. Watzlawik J, Skora L, Frense D, Griesinger C, Zweckstetter M, Schulz-Schaeffer WJ, Kramer ML (2006) Prion protein helix1 promotes aggregation but is not converted into beta-sheet. J Biol Chem 281:30242–30250
23. Chatterjee B, Lee CY, Lin C, Chen EH, Huang CL, Yang CC, Chen RP (2013) Amyloid core formed of full-length recombinant mouse prion protein involves sequence 127–143 but not sequence 107–126. PLoS ONE 8:e67967
24. Muramoto T, Scott M, Cohen FE, Prusiner SB (1996) Recombinant scrapie-like prion protein of 106 amino acids is soluble. Proc Natl Acad Sci USA 93:15457–15462
25. Shindoh R, Kim CL, Song CH, Hasebe R, Horiuchi M (2009) The region approximately between amino acids 81 and 137 of proteinase K-resistant PrPSc is critical for the infectivity of the Chandler prion strain. J Virol 83:3852–3860
26. Chabry J, Caughey B, Chesebro B (1998) Specific inhibition of in vitro formation of protease-resistant prion protein by synthetic peptides. J Biol Chem 273:13203–13207
27. Chabry J, Priola SA, Wehrly K, Nishio J, Hope J, Chesebro B (1999) Species-independent inhibition of abnormal prion protein (PrP) formation by a peptide containing a conserved PrP sequence. J Virol 73:6245–6250
28. DeMarco ML, Daggett V (2004) From conversion to aggregation: protofibril formation of the prion protein. Proc Natl Acad Sci USA 101:2293–2298
29. DeMarco ML, Silveira J, Caughey B, Daggett V (2006) Structural properties of prion protein protofibrils and fibrils: an experimental assessment of atomic models. Biochemistry 45:15573–15582
30. Chen PY, Lin CC, Chang YT, Lin SC, Chan SI (2002) One O-linked sugar can affect the coil-to-b structural transition of the prion peptide. Proc Natl Acad Sci USA 99:12633–12638
31. Liao Y-D, Jeng J-C, Wang C-F, Wang S-C, Chang S-T (2004) Removal of N-terminal methionine from recombinant proteins by engineered E. coli methionine aminopeptidase. Prot Sci 13:1802–1810
32. Dalboge H, Bayne S, Pedersen J (1990) In vivo processing of N-terminal methionine in *E. coli*. FEBS Lett 266:1–3
33. Sang JC, Lee CY, Luh FY, Huang YW, Chiang YW, Chen RP (2012) Slow spontaneous α-to-β structural conversion in a non-denaturing neutral condition reveals the intrinsically disordered property of the disulfide-reduced recombinant mouse prion protein. Prion 6:489–497
34. Krebs MRH, Bromley EHC, Donald AM (2005) The binding of thioflavin-T to amyloid fibrils: localisation and implications. J Struct Biol 149:30–37
35. Khurana R, Coleman C, Ionescu-Zanetti C, Carter SA, Krishna V, Grover RK, Roy R, Singh S (2005) Mechanism of thioflavin T binding to amyloid fibrils. J Struct Biol 151:229–238
36. Hsu JC, Chen HL, Snoeberger RC, Luh FY, Lim TS, Hsu C, Chen RP (2013) Thioflavin T and its photo-irradiative derivatives: Exploring their spectroscopic properties in the absence and presence of amyloid fibrils. J Phys Chem B 117:3459–3468
37. Lee LY, Chen RP (2007) Quantifying the sequence-dependent species barrier between hamster and mouse prions. J Am Chem Soc 129:1644–1652
38. Singh J, Kumar H, Sabareesan AT, Udgaonkar JB (2014) Rational stabilization of helix 2 of the prion protein prevents its misfolding and oligomerization. J Am Chem Soc 136:16704–16707

39. Yamaguchi K, Matsumoto T, Kuwata K (2008) Critical region for amyloid fibril formation of mouse prion protein: unusual amyloidogenic properties of the helix 2 peptide. Biochemistry 47:13242–13251
40. Priola SA, Chesebro B (1995) A single hamster PrP amino acid blocks conversion to protease-resistant PrP in scrapie-infected mouse neuroblastoma cells. J Virol 69:7754–7758
41. Vanik DL, Surewicz KA, Surewicz WK (2004) Molecular basis of barriers for interspecies transmissibility of mammalian prions. Mol Cell 14:139–145
42. Jones EM, Surewicz WK (2005) Fibril conformation as the basis of species- and strain-dependent seeding specificity of mammalian prion amyloids. Cell 121:63–72
43. Theint T, Nadaud PS, Aucoin D, Helmus JJ, Pondaven SP, Surewicz K, Surewicz WK, Jaroniec CP (2017) Species-dependent structural polymorphism of Y145Stop prion protein amyloid revealed by solid-state NMR spectroscopy. Nat Commun 8:753
44. Groveman BR, Dolan MA, Taubner LM, Kraus A, Wickner RB, Caughey B (2014) Parallel in-register intermolecular beta-sheet architectures for prion-seeded prion protein (PrP) amyloids. J Biol Chem 289:24129–24142
45. Wille H, Bian W, McDonald M, Kendall A, Colby DW, Bloch L, Ollesch J, Borovinskiy AL, Cohen FE, Prusiner SB, Stubbs G (2009) Natural and synthetic prion structure from X-ray fiber diffraction. Proc Natl Acad Sci USA 106:16990–16995
46. Silva CJ, Vazquez-Fernandez E, Onisko B, Requena JR (2015) Proteinase K and the structure of PrPSc: the good, the bad and the ugly. Virus Res 207:120–126
47. Wille H, Requena JR (2018) The Structure of PrP(Sc) Prions. Pathogens 7
48. Govaerts C, Wille H, Prusiner SB, Cohen FE (2004) Evidence for assembly of prions with left-handed β-helices into trimers. Proc Natl Acad Sci USA 101:8342–8347